



# Development of an Association Technique for a 3-Dimensional Minimum Configuration Multilateration System

Abdulmalik Shehu Yaro<sup>1\*</sup>, Ahmad Zuri Sha'ameri<sup>2</sup>

<sup>1</sup>Department of Electronics and Telecommunications Engineering Ahmadu Bello University (ABU), Zaria, NIGERIA

<sup>2</sup>School of Electrical Engineering  
University Teknologi Malaysia (UTM), Skudai, 81310, MALAYSIA

\*Corresponding Author

DOI: <https://doi.org/10.30880/ijie.2020.12.01.006>

Received 22 October 2018; Accepted 7 February 2019; Available online 31 January 2020

**Abstract:** Multilateration (MLAT) system estimates the position of an aircraft using time difference of arrival (TDOA) measurement estimated at ground receiving station (GRS) pairs with a lateration algorithm. In a multiple aircraft scenario, multiple TDOA measurements are estimated at GRS pairs. Thus, there is a need to group and associate the TDOA measurements according to each aircraft before the position estimation (PE) process with the lateration algorithm. In this paper, a multi-reference TDOA association (M-RETA) technique based on multiple referencing approach to TDOA estimation, its zero cyclic sum property and nearest neighbour search approach is developed for a minimum configuration 3-D MLAT system. The performance of the M-RETA technique is determined considering a five aircraft flying configuration with an aircraft pair separation of at least 5.5 km in accordance to the Federal Aviation Administration (FAA) standard. Simulation result shows that the M-RETA technique association accuracy depends on the TDOA estimation error and separation between the aircraft. Simulation result shows that the M-RETA technique as on an average 88% probability of correct association.

**Keywords:** TDOA, zero cyclic sum, nearest neighbor search, association

## 1. Introduction

Multilateration (MLAT) system is one of the surveillance systems used by an air navigation service provider (ANSP) to track aircraft within its flight information region (FIR) (ICAO, 2007). The system first estimates time difference of arrival (TDOA) measurement from the aircraft transponder replies such as the automatic surveillance dependent broadcast (ADS-B) signals captured by ground receiving station (GRS) pairs (ICAO, 2007; Kaune, Steffes, Rau, Konle, & Pagel, 2012; Shamian, Hadi, & Ijaz, 2012). These TDOA measurements are used with the known coordinate of the deployed GRSs as inputs to a lateration algorithm which then estimates the position of the aircraft. There is a nonlinear relationship between the input variable (TDOA measurement) to the lateration algorithm and output variable (aircraft position) (Gaspere Galati, Leonardi, Balbastre-Tejedor, & Mantilla-Gaviria, 2014; Yaro & Sha'ameri, 2018). To obtain the aircraft position, there is a need to establish a linear relationship between the two variables. For this reason, several approaches have been developed which can be grouped as closed-form and open form approaches (So, 2012; Yaro, Sha'ameri, & Kamel, 2018). In the open form approach, linearization algorithms are used to obtain the linear relationship between the two variables (Gaspere Galati et al., 2014; So, 2012). This is followed by an iteration process with an input random aircraft position while minimizing a maximum likelihood function. The open form approach suffers convergence if the initial random aircraft position is far from the actual aircraft position (Chaitanya, Kumar, Rao, & Goswami, 2015). Algebraic manipulations are used in the closed-form approach to obtain the linear relationship between the two variables

(Weng, Xiao, & Xie, 2011; Yaro, Sha'ameri, & Kamel, 2017). It does not suffer convergence issue as on randomly input aircraft position is used but very sensitive to error in the input variable (Yaro et al., 2018). The closedform approach to the development of the lateration algorithm is mostly used in passive real time system which the MLAT system is an example. For this reason, the closed-form approach to the lateration algorithm is adopted in this paper.

Several aircraft exist within the FIR assigned to an ANSP which result in multiple TDOA measurements estimated at GRS pairs (Scheuing & Yang, 2008). To estimate each aircraft position, the TDOA measurements obtained from GRS pairs need to be grouped according to aircraft in a process called TDOA measurement association. Several articles have reported on different approaches to TDOA measurements association (Amishima, Wakayama, & Okamura, 2014; Herath, Pathirana, Champion, & Ekanayake, 2012; Jamali-Rad & Leus, 2013; Lee, Lee, Yang, Lee, & Hwang, 2016; Li & Li, 2014; Xionghu Zhong & Hopgood, 2015). According to (Herath et al., 2012), a minimum of four GRSs is required to uniquely localize more than one aircraft using the MLAT system within the FIR of a ANSP. A fingerprinting TDOA measurement based association technique is developed in (Jamali-Rad & Leus, 2013). Every aircraft position has a unique TDOA measurement set. A database is developed that contains predetermined TDOA measurement set of an aircraft at several positions within the defined MLAT system coverage. The association technique developed in (Li & Li, 2014) is based on the nearest neighbour search algorithm and on the assumption that multiple TDOA measurements of an aircraft are available within a single observation window. Beside associating the TDOA measurements to the aircraft, some techniques first associate the signals to each aircraft afterwards obtain the TDOA measurements (Xu, Chen, & Jiang, 2013). This is possible if some unique properties related to each aircraft can be derived from the signal such as carrier frequency, modulation type, pulse width and pulse amplitude.

In this paper, a multi-reference TDOA association (M-RETA) technique is developed under the assumption that all TDOA measurements are obtained at a single time instance from multiple aircraft all operating at the same downlink frequency. It is based on multiple referencing approach to TDOA estimation using a total of four deployed GRSs, TDOA measurement zero cyclic sum property and nearest neighbour search approach. The M-RETA technique is verified considering an aircraft configuration with a minimum aircraft pair separation of 5.5 km in accordance with the FAA horizontal separation standard (Sha'ameri, Yaro, Amjad, & Hamdi, 2017). After the TDOA measurements have been associated to each aircraft, their positions are obtained using the multiple reference closed-form lateration algorithm developed in (Yaro et al., 2017).

The remainder of the paper is organized as follows: Section 2 gives a description on the TDOA measurement estimation considering multiple aircraft. This is followed by the methodology for the developed M-RETA technique, the condition for TDOA measurement association error and a brief description on multiple reference closed-form lateration algorithm developed in (Yaro et al., 2017). The simulation result and discussion presented in Section 4 and finally the conclusion in Section 5.

## 2. TDOA Measurement Estimation in Multiple Aircraft Scenario

Within an observation window, signals from multiple aircraft are captured at all deployed GRSs resulting in multiple TDOA measurements between GRS pairs. The information contained in each signal such as aircraft identification, position and aircraft velocity are different. Thus, the assumption of statistical independence of signals from different aircraft is valid. Therefore, for  $N$  observed aircraft,  $N$  TDOA measurements are estimated by each GRS pair.

For simplicity, consider the  $(n - 1) - th$  and the  $n - th$  aircraft with coordinates  $\mathbf{x}_{e,n-1} = (x_{e,n-1}, y_{e,n-1}, z_{e,n-1})$  and  $\mathbf{x}_{e,n} = (x_{e,n}, y_{e,n}, z_{e,n})$  respectively. Within an observation window of  $0 \leq t \leq T$ , the signal transmitted by these aircrafts are captured at two GRSs labelled  $i - th$  and  $m - th$  with coordinates as shown in Fig. 1.

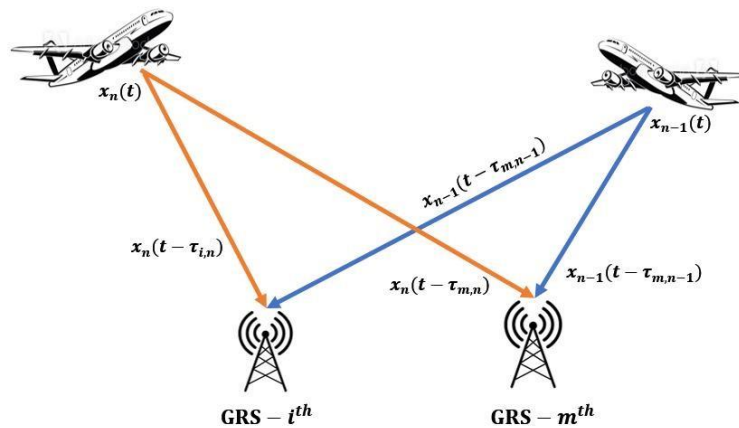


Fig. 1 - TDOA measurements from multiple aircraft scenario.

The signals at the  $i$ -th and  $m$ -th GRS pair can be mathematically expressed as:

$$x_i(t) = x_{n-1}(t - \tau_{i,n-1}) + x_n(t - \tau_{i,n}) \tag{1a}$$

$$x_m(t) = x_{n-1}(t - \tau_{m,n-1}) + x_n(t - \tau_{m,n}) \tag{1b}$$

where  $\tau_{i,n-1}$  and  $\tau_{i,n}$  are the time of arrival (TOA)s in second of signal transmitted by the  $n - th$  and  $(n - 1) - th$  aircrafts respectively detected at the  $i$ -th GRS while  $\tau_{m,n-1}$  and  $\tau_{m,n}$  are the TOAs of signal transmitted by the  $n - th$  and  $(n - 1) - th$  aircrafts respectively at the  $m$ -th GRS. The TOA is the time taken by the signal to propagate from the aircraft to the GRS.

The peak of the result of the cross-correction between  $x_i(t)$  and  $x_m(t)$  in Eq. (1) is (Marmaroli, Falourd, & Lissek, 2012):

$$R_{im}(\tau) = R(\tau - \tau_{im,n-1}) + R(\tau - \tau_{im,n}) \tag{2}$$

where:

$$\tau_{im,n-1} = \tau_{i,n-1} - \tau_{m,n-1} \tag{3a}$$

$$\tau_{im,n} = \tau_{i,n} - \tau_{m,n} \tag{3b}$$

are the TDOA measurement of the  $(n - 1) - th$  and  $n - th$  aircraft respectively obtain using the  $i$ -th and  $m$ -th GRS pair.

The TDOA measurements in Eq. (3) can be put in a vector form as follows:

$$\mathbf{T}_{im} = [\tau_{im,n-1}, \tau_{im,n}] \tag{4}$$

Noise present in the received signal results in TDOA measurement error. By modelling the TDOA error as a zero mean Gaussian random variable with probability density function (pdf) as  $N(0, \sigma)$ , the estimated TDOA measurement vector in Eq. (3) is written as:

$$\mathbf{T}_{im} = [\hat{\tau}_{im,n-1}, \hat{\tau}_{im,n}] \tag{5}$$

where

$$\hat{\tau}_{im,n-1} = \tau_{im,n-1} + N(0, \sigma_{n-1}) \tag{6a}$$

$$\hat{\tau}_{im,n} = \tau_{im,n} + N(0, \sigma_n) \tag{6b}$$

and  $\sigma_{n-1}$  and  $\sigma_n$  are the TDOA error standard deviation (SD)s in obtaining the TDOAs of the  $(n - 1) - th$  and  $n - th$  aircrafts which depends in the SNR of the signal transmitted by either aircraft detected at the  $i$ -th and  $m$ -th GRSs. For the  $n - th$  aircraft, the  $\sigma_n$  in second is related to the SNR in dB as (G. Galati, Leonardi, Mantilla-Gaviria, & Tosti, 2012):

$$\sigma_n(s) \cong \frac{3}{B\sqrt{2}} \times \sqrt{\left(10^{-(0.1 \times SNR_i^n)} + 10^{-(0.1 \times SNR_m^n)}\right)} \tag{7}$$

where  $B$  is the bandwidth of the receiver in Hz,  $SNR_i^n$  and  $SNR_m^n$  respectively are the received SNR at  $i$ -th and  $m$ -th GRS pair of the signal transmitted by the  $n - th$  aircraft.

With a total of  $L$  GRSs, the number of TDOA measurement vectors in the form of Eq. (5) depends on the number of GRSs used as reference for estimating the TDOA measurements. For instance, using single GRS as reference will result in  $L - 1$  TDOA measurement vectors (Mantilla-Gaviria, Leonardi, Galati, & Balbastre-Tejedor, 2015). To obtain the position of all  $N$  aircrafts, there is a need to associate the TDOA measurements from all GRS pairs to each aircraft. The TDOA measurements identified to belong the same aircraft are subsequently sent to the lateration algorithm for use to estimate the aircraft position. In the next section, the methodology for the proposed M-RETA technique is presented.

### 3. Methodology

In this section, a detail description of the proposed M-RETA technique is presented with is followed by the condition for TDOA measurement association error. Finally, a brief description on multiple reference closed-form lateration algorithm used in the position estimation (PE) of the aircraft.

#### 3.1 M-RETA Technique Development

As stated earlier, 3-D multilateration system with the minimum configuration is considered. Let there be a total of  $N$  aircrafts within the flight information region and a copy of the signal from each aircraft is captured within the observation window. With the  $i$ -th and  $j$ -th GRS pair as reference, the generated TDOA measurement vector with the  $m$ -th and  $k$ -th as non-reference GRS in the form of Eq. (5) are described as follows:

$$\mathbf{T}_{im} = [\hat{\tau}_{im,1}, \hat{\tau}_{im,2}, \dots, \hat{\tau}_{im,N}] \tag{8}$$

$$\mathbf{T}_{jm} = [\hat{\tau}_{jm,1}, \hat{\tau}_{jm,2}, \dots, \hat{\tau}_{jm,N}] \tag{9}$$

$$\mathbf{T}_{ik} = [\hat{\tau}_{ik,1}, \hat{\tau}_{ik,2}, \dots, \hat{\tau}_{ik,N}] \tag{10}$$

$$\mathbf{T}_{jk} = [\hat{\tau}_{jk,1}, \hat{\tau}_{jk,2}, \dots, \hat{\tau}_{jk,N}] \tag{11}$$

where  $i \neq m \neq j \neq k$  and  $n = [1, 2, \dots, N]$ .

Using Eq. (8) and Eq. (9), a TDOA difference matrix can be obtained as follows:

$$\mathbf{T}_{ijm} = \begin{bmatrix} a_{1,1} & \dots & a_{1,v} \\ \vdots & \ddots & \vdots \\ a_{u,1} & \dots & a_{u,v} \end{bmatrix} \tag{12a}$$

where

$$a_{u,v} = \hat{\tau}_{im,u} - \hat{\tau}_{jm,v} \tag{12b}$$

for  $1 \leq u \leq N, 1 \leq v \leq N, \hat{\tau}_{im,u} \in \mathbf{T}_{im}$  and  $\tau_{jm,v} \in \mathbf{T}_{jm}$

Another TDOA difference matrix can be obtained using Eq. (10) and Eq. (11) as follows:

$$\mathbf{T}_{ijk} = \begin{bmatrix} b_{1,1} & \dots & b_{1,p} \\ \vdots & \ddots & \vdots \\ b_{o,1} & \dots & b_{o,p} \end{bmatrix} \tag{13a}$$

where

$$b_{o,p} = \hat{\tau}_{ik,o} - \hat{\tau}_{jk,p} \tag{13b}$$

for  $1 \leq o \leq N, 1 \leq p \leq N, \hat{\tau}_{ik,o} \in \mathbf{T}_{ik}$  and  $\tau_{jk,p} \in \mathbf{T}_{jk}$

The matrix  $\mathbf{T}_{ijm}$  is obtained using the TDOA vector  $\mathbf{T}_i$  and  $\mathbf{T}_{jm}$  while matrix  $\mathbf{T}_{ijk}$  is obtained using the TDOA vectors  $\mathbf{T}_{ik}$  and  $\mathbf{T}_{jk}$ . The entries of these matrices are element-wise subtraction between the two vectors used in obtaining them. Consider the TDOA measurement vector pair  $im$  and  $\mathbf{T}_{jm}$  in Eq. (8) and Eq. (9) respectively and let  $\tau_{im,n} \in \mathbf{T}_{im}$  and  $\tau_{jm,n} \in \mathbf{T}_{jm}$  be the TDOA measurement of the  $n$ -th emitter. The difference between  $\tau_{im,n}$  and  $\tau_{jm,n}$  will result in another TDOA measurement  $\tau_{ij,n}$  as follows:

$$\tau_{im,n} - \tau_{jm,n} = \tau_{ij,n} \tag{14}$$

Expanding the left-hand side of Eq. (14) will result in:

$$\tau_{i,n} - \tau_{m,n} - \tau_{j,n} + \tau_{m,n} = \tau_{ij,n} \tag{15b}$$

$$\tau_{i,n} - \tau_{j,n} = \tau_{ij,n} \tag{15c}$$

$$\tau_{ij,n} = \tau_{ij,n} \tag{15d}$$

From Eq. (15d), the left-hand side of the equation is equals to the right-hand side of the equation. Based on the TDOA measurement zero cyclic sum property defined in (Scheuing & Yang, 2008), the TDOA measurements  $\tau_{im}, \tau_{jm},n$  and  $\tau_{ij,n}$  in Eq. (14) belongs to the  $n -$  th aircraft. This is also the same for the TDOA measurement vector pair  $\mathbf{T}_{ik}$  and  $\mathbf{T}_{jk}$  in Eq. (10) and Eq. (11) respectively in which

$$\tau_{ik,n} - \tau_{jk,n} = \tau_{ij,n} \tag{16}$$

$$\tau_{ij,n} \in \mathbf{T}_{ij} \tag{17}$$

where  $\tau_{ik,n} \in \mathbf{T}_{ik}$  and  $\tau_{jk,n} \in \mathbf{T}_{jk}$

If the result from the left-hand side in Eq. (15d) is the same as that in Eq. (16), it means that  $\tau_{ik,n}$ , and  $\tau_{jk,n}$  also belongs to the  $n -$  th aircraft. The TDOA measurement  $\tau_{ij}$  in Eq. (14) and Eq. (16) can be seen to be obtained using the  $i$ -th and  $j$ -th GRS which are earlier considered as the reference GRS for the TDOA estimation. Thus, another TDOA measurement vector,  $\mathbf{T}_{ij}$  using the  $i$ -th and  $j$ -th GRS is then obtained thus,

Based on Eq. (12) to Eq. (17), it can be concluded that

$$\mathbf{T}_{ij} \subseteq \mathbf{T}_{ijm} \tag{18}$$

$$\mathbf{T}_{ij} \subseteq \mathbf{T}_{ijk} \tag{19}$$

To associate the TDOA measurement to an aircraft whose TDOA measurements are in the vectors  $\mathbf{T}_{im}, \mathbf{T}_{jm}, \mathbf{T}_{ik}, \mathbf{T}_{jk}$  and  $\mathbf{T}_{ij}$ , take the first entry of TDOA vector  $\mathbf{T}_{ij}$  and search for this value in matrices  $\mathbf{T}_{ijm}$  and  $\mathbf{T}_{ijk}$  in Eq. (12) and Eq. (13) respectively. Due to error in the TDOA measurements, the likelihood of finding the exact value in the matrices  $\mathbf{T}_{ijm}$  and  $\mathbf{T}_{ijk}$  is very low. A possible way is the use of the nearest neighbor search approach in which the pair of TDOA measurements with the least residual are said to be the same. For this reason, a residual matrix is generated using the selected TDOA measurement from the vector  $\mathbf{T}_{ij}$ . The residual matrices for the  $n -$  th TDOA measurement,  $\hat{\tau}_{ij,n} \in \mathbf{T}_{ij}$  generated using matrices  $\mathbf{T}_{ijm}$  and  $\mathbf{T}_{ijk}$  in Eq. (12) and Eq. (13) respectively are as follows:

$$\Delta \mathbf{T}_{ijm} = \begin{bmatrix} c_{1,1} & \cdots & c_{1,v} \\ \vdots & \ddots & \vdots \\ c_{u,1} & \cdots & c_{u,v} \end{bmatrix} \tag{20}$$

$$\Delta \mathbf{T}_{ijk} = \begin{bmatrix} d_{1,1} & \cdots & d_{1,p} \\ \vdots & \ddots & \vdots \\ d_{o,1} & \cdots & d_{o,p} \end{bmatrix} \tag{21}$$

where

$$c_{u,v} = \left| \hat{\tau}_{ij,n} - a_{u,v} \right| \tag{22a}$$

$$d_{o,p} = \left| \hat{\tau}_{ij,n} - b_{o,p} \right| \tag{22b}$$

The  $c_u$ , and  $d_{o,p}$  in Eq. (22) with the least value are nearest to  $\hat{\tau}_{ij,n}$ . The TDOA measurement pairs in the matrices  $\mathbf{T}_{ijm}$  and  $\mathbf{T}_{ijk}$  in Eq. (12b) and Eq. (13b) used in obtaining  $c_u$ , and  $d_{o,p}$  in Eq. (22) belongs to the same aircraft. These TDOA measurements are subsequently sent to the localization algorithm for the PE. Summary of the proposed TDOA measurements association algorithm is as follows:

- i. Generate the matrices  $\mathbf{T}_{ijm}$  and  $\mathbf{T}_{ijk}$  in Eq. (12) and Eq. (13) respectively.
- ii. Take the first TDOA measurement entry in the  $\mathbf{T}_{ij}$  vector and generate the residual matrices in Eq. (20) and Eq. (21).
- iii. Select the TDOA measurements  $a_u$ , and  $b_o$ , from Eq. (22) that resulted in the entries of the residual matrices in Eq. (20) and Eq. (21) with the least value.
- iv. Identify the TDOA measurement pair subtracted used to generate  $a_u$ , and  $b_o$ , from (iii) using Eq. (12b) and Eq. (13b) respectively.
- v. The two pairs of TDOA measurements from (iv) belongs to the same aircraft which are subsequently sent to the lateration algorithm to obtain it position.
- vi. Take the second entry of the  $\mathbf{T}_{ij}$  and repeat (ii) to (v) to estimate the position of the second aircraft. Continue (ii) to (v) till all entries in the vector  $\mathbf{T}_{ij}$  are used.

### 3.2 TDOA Measurement Association Error Condition and Probability

The TDOA measurements in Eq. (5) are obtained without knowledge which TDOA measurement belongs to which aircraft. Due to the geometrical relationship between TDOA measurement and aircraft location, closely spaced aircraft will have their estimated TDOA measurements close together. This will increase the likelihood of the two TDOA measurements to be miss-associated resulting to a TDOA association error. A TDOA association error occurs when TDOA measurement which does not belong to an aircraft is identified to belong to that aircraft. This usually occur when the aircraft are closely spaced to the extent that their TDOA error probability density distribution (PDF)s have an overlapping region (region A and region B) as shown in Fig. 2.

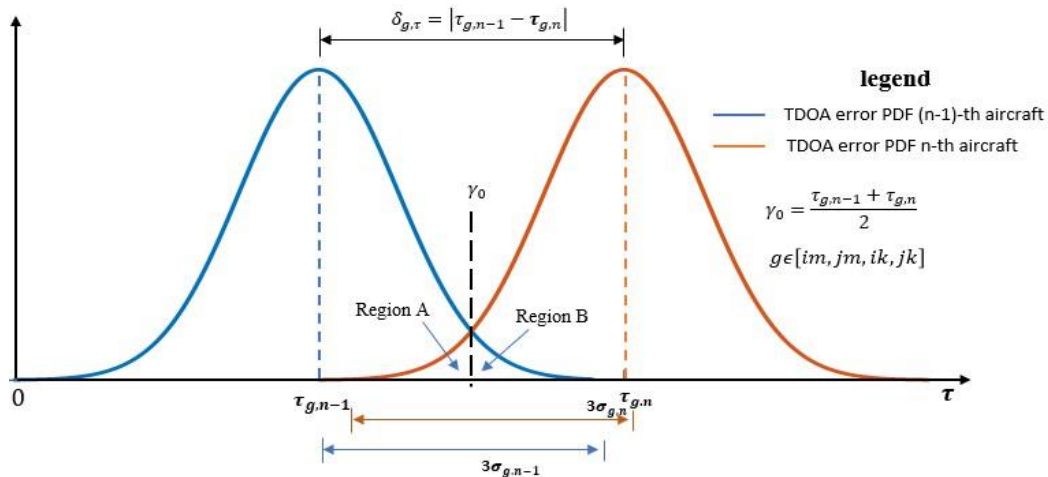


Fig. 2 - TDOA error PDF distribution of the  $(n - 1) - \text{th}$  and  $n - \text{th}$  aircraft

The PDFs shown in Fig. 2 are mathematically expressed as:

$$p(\tau | \tau_{g,n-1}) = \frac{1}{\sigma_{g,n-1} \sqrt{2\pi}} \exp \left[ -\frac{1}{2} \left( \frac{\tau - \tau_{g,n-1}}{\sigma_{g,n-1}} \right)^2 \right] \text{ for } g \in [im, jm, ik, jk] \quad (23)$$

$$p(\tau | \tau_{g,n}) = \frac{1}{\sigma_{g,n} \sqrt{2\pi}} \exp \left[ -\frac{1}{2} \left( \frac{\tau - \tau_{g,n}}{\sigma_{g,n}} \right)^2 \right] \quad (24)$$

Given the TDOA error SDs and the mean TDOA values, Eq. (25) is used to determine if the overlapping region given as region A and region B as shown in Fig. 2 is created.

$$\delta_{g,\tau} = |\tau_{g,n-1} - \tau_{g,n}| < 3(\sigma_{g,n-1} + \sigma_{g,n}) \tag{25}$$

If the absolute difference between the mean TDOAs of the  $(- 1) -$  th and  $n -$  th aircraft is less than the three times the summation of the TDOA error SDs, the overlapping region is created. After it is determined that the overlapping region is created, next is to determine the probability of TDOA association error. This is given by the area of the overlapping region. The area of the overlapping region A from Fig. 2 is mathematically obtained as:

$$P(e|\tau_{g,n-1}) = P(\hat{\tau}_{g,n}|\tau_{g,n-1}) = \int_{\gamma_0}^{\infty} p(\tau|\tau_{g,n-1})d\tau \tag{26}$$

and that of region B is:

$$P(e|\tau_{g,n}) = P(\hat{\tau}_{g,n-1}|\tau_{g,n}) = \int_{-\infty}^{\gamma_0} p(\tau|\tau_{g,n})d\tau \tag{27}$$

Thus, the TDOA association error probability for a given TDOA measurement vector is mathematically obtained as:

$$P_{assoc\_error}^g = P(e|\tau_{g,n-1}) + P(e|\tau_{g,n}) \tag{28}$$

The PE error obtained by the lateration algorithm is either due to the TDOA association error of the M-RETA technique and or TDOA estimation error. Therefore, the probability that the PE error obtained by the lateration algorithm is due the TDOA association error is mathematically obtained as:

$$P_{PE\_assoc\_error} = \frac{1}{4} \times (P_{assoc\_error}^{im} + P_{assoc\_error}^{jm} + P_{assoc\_error}^{ik} + P_{assoc\_error}^{jk}) \tag{30}$$

while the probability that the PE error is due to TDOA estimation error is:

$$P_{PE\_TDOA\_error} = 1 - P_{PE\_assoc\_error} \tag{31}$$

The Eq. (30) and Eq. (31) are to be used to determine the performance of the M-RETA technique presented in Subsection 3.1 when coupled with the lateration algorithm.

### 3.3 Multiple reference closed-form lateration algorithm

After the TDOA measurements for each aircraft has been identified, the next step is to estimate the position of the aircraft. Let  $\tau_{im,n}$ ,  $\tau_{jm,n}$ ,  $\tau_{ik,n}$ , and  $\tau_{jk,n}$  be the grouped the TDOA measurement obtained by the M-RETA technique for the  $n -$  th aircraft. The TDOA measurements are related to the aircraft positions as follows:

$$\tau_{im,n} = \frac{1}{c} \left( \begin{array}{l} \sqrt{(x_{e,n} - x_i)^2 + (y_{e,n} - y_i)^2 + (z_{e,n} - z_i)^2} \\ -\sqrt{(x_{e,n} - x_m)^2 + (y_{e,n} - y_m)^2 + (z_{e,n} - z_m)^2} \end{array} \right) \quad (32)$$

$$\tau_{jm,n} = \frac{1}{c} \times \left( \begin{array}{l} \sqrt{(x_{e,n} - x_j)^2 + (y_{e,n} - y_j)^2 + (z_{e,n} - z_j)^2} \\ -\sqrt{(x_{e,n} - x_m)^2 + (y_{e,n} - y_m)^2 + (z_{e,n} - z_m)^2} \end{array} \right) \quad (33)$$

$$\tau_{ik,n} = \frac{1}{c} \times \left( \begin{array}{l} \sqrt{(x_{e,n} - x_i)^2 + (y_{e,n} - y_i)^2 + (z_{e,n} - z_i)^2} \\ -\sqrt{(x_{e,n} - x_k)^2 + (y_{e,n} - y_k)^2 + (z_{e,n} - z_k)^2} \end{array} \right) \quad (34)$$

$$\tau_{jk,n} = \frac{1}{c} \times \left( \begin{array}{l} \sqrt{(x_{e,n} - x_j)^2 + (y_{e,n} - y_j)^2 + (z_{e,n} - z_j)^2} \\ -\sqrt{(x_{e,n} - x_k)^2 + (y_{e,n} - y_k)^2 + (z_{e,n} - z_k)^2} \end{array} \right) \quad (35)$$

where:  $\mathbf{x}_{e,n} = (x_{e,n}, y_{e,n}, z_{e,n})$  is the location of the  $n$ -th aircraft;  $c = 3 \times 10^9$ , while  $\mathbf{s}_i = (x_i, y_i, z_i)$ ,  $\mathbf{s}_j = (x_j, y_j, z_j)$ ,  $\mathbf{s}_m = (x_m, y_m, z_m)$  and  $\mathbf{s}_k = (x_k, y_k, z_k)$  respectively are the locations of the  $i$ -th,  $j$ -th,  $k$ -th and  $m$ -th GRSs.

Algebraically manipulating Eq. (32) to Eq. (35) as previously done in (Yaro et al., 2017) results in a pair of 3-D plane equations presented as follows:

$$A_{ijm} = x_{e,n} B_{ijm} + y_{e,n} C_{ijm} + z_{e,n} D_{ijm} \quad (37)$$

$$A_{ijk} = x_{e,n} B_{ijk} + y_{e,n} C_{ijk} + z_{e,n} D_{ijk} \quad (38)$$

where the coefficients of Eq. (37) and Eq. (38) are functions of the TDOA measurements and GRS coordinates which can be found in (Yaro et al., 2017).

The subscript “ $ijm$ ” and “ $ijk$ ” in the coefficients of Eq. (37) and Eq. (38) respectively indicates that the resulting variable is from the measurements obtained using the  $i$ -th and  $j$ -th GRS as reference station respectively with the  $m$ -th or  $k$ -th as non-reference GRSs. A detailed derivation of Eq. (37) to Eq. (38) and how the coordinates of the aircrafts are obtained using the pair of equations can be found in (Yaro et al., 2017).

## 4 Simulation Result and Discussion

The performance of the M-RETA technique developed in sub-section 3.1 presented in this section of the paper. Its performance is presented in terms of probability of correct PE based on Eq. (30) and Eq. (31). Firstly, the simulation parameter is presented which is followed by the variation of the TDOA error SD with the aircraft position. The probability of correct PE by the M-RETA technique is subsequently presented and lastly, the PE error obtained by multiple reference closed-form lateration algorithm is presented.

### 4.1 Simulation Parameter

The performance of the M-RETA technique is evaluated considering civil aviation surveillance. The system parameters which include that of the aircraft transponder and ground station system is presented in Table 1.

**Table 1 - Aircraft transponder and ground station system parameters**

	Parameter	Values
Aircraft transponder	Antenna gain Peak	3 dBi
	transmit power	250 W
	Operating frequency	1090 MHz
Ground system	Antenna gain	12 dBi
	Sensitivity	-95 dBm
	Antenna height	200 m
	Receiver bandwidth	20 MHz

A five-square aircraft flying configuration is considered in evaluating the performance of the M-RETA technique with a minimum horizontal lateration separation of about 5.5 km in accordance with FAA standard. Fig. 4 shows the geometrical position of each aircraft while Table 2 shows the position of each rectangular coordinate system. The minimum separation between any given aircraft pair based on the configuration shown in Fig. 3 is 5.5 km which is between aircraft A and any of the remaining aircraft.

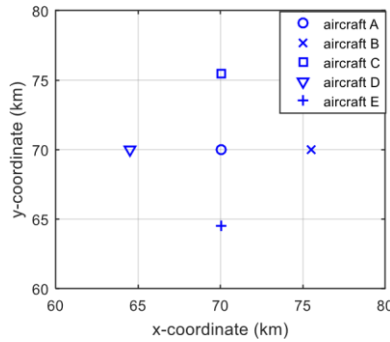


**Fig. 3 - The five-square aircraft flying configuration geometrical positions**

**Table 2 - Aircraft positions in rectangular coordinate system**

Aircraft	Position		
	<i>x</i> (km)	<i>y</i> (km)	<i>z</i> (km)
A	70	70	
B	75.5	70	
C	70	75.5	7
D	64.5	70	
E	70	64.5	

The configuration of the deployed GRSs contributes to the PE accuracy of the aircraft PE algorithm presented in section 3.3. According to Chan *et al* (Chen, Francisco, Trappe, & Martin, 2006), the best configuration for a total number of 4 GRSs is the square configuration and in this research, the 10-km square shape GRS configuration is adopted with each GRS at the vertex (Yaro & Sha’ameri, 2018; Yaro et al., 2017). The distribution of the GRSs are shown in Fig. 4.

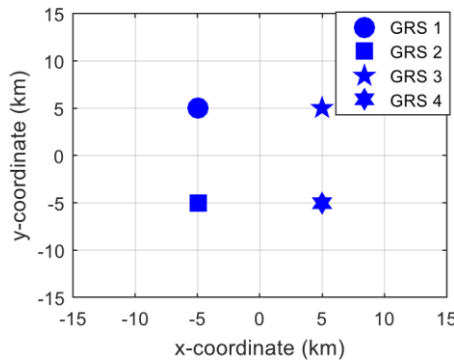


**Fig. 4 - Distribution of the GRS in square configuration**

The five-square flying aircraft configuration considered in this paper for the analysis can be seen to be on the top right quadrant of the GRS four square configuration. It is presented in (Yaro et al., 2017) that the choice of GRS reference pair for TDOA estimation contributes to the PE accuracy of the lateration algorithm. The best GRS pair to use as reference to estimate the position of the aircraft in the top right quadrant of the GRS configuration as shown in Fig. 4 is GRS pair 1 and 4 that is  $i = 1$  and  $j = 4$ . Thus, all the possible combination of GRS pairs to generate the TDOA measurement vectors in Eq. (8) to Eq. (11) are shown in Table 3.

**Table 3- All possible GRS pair generation of TDOA measurement vector**

GRS pair		Non-reference GRS pair	
		$k = 2$	$k = 3$
Reference	$i = 1$	Pair 1	Pair 2
GRS pair	$j = 4$	Pair 3	Pair 4

**4.1 Variation of TDOA Error SD with Aircraft Position**

At 7 km altitude, there is line of sight between each aircraft to all the GRSs for this reason, the free space path loss model is considered for the SNR calculation. Using Eq. (7), the TDOA error SD of each aircraft obtained using each of the GRS pair combination presented in Table 3 is shown in Table 4.

**Table 4 - TDOA error SD for different GRS pair combination**

Aircraft	TDOA SD at GRS pair position (nsec)			
	Pair 1	Pair 2	Pair 3	Pair 4
A	2.55	2.45	2.65	2.55
B	2.86	2.77	2.95	2.86
C	2.46	2.36	2.55	2.46
D	2.26	2.17	2.35	2.26
E	2.66	2.57	2.75	2.66

Based on the aircraft configuration shown in Fig. 3 and using the system parameter as shown Table 1, the maximum TDOA error SD is 2.95 nsec and the minimum is 2.17 nsec. The graphical representation of the error free TDOA measurement vectors that is  $T_{12}$ ,  $T_{13}$ ,  $T_{42}$  and  $T_{43}$  based on the aircraft flying configuration in Fig. 3 is shown in Fig. 5.

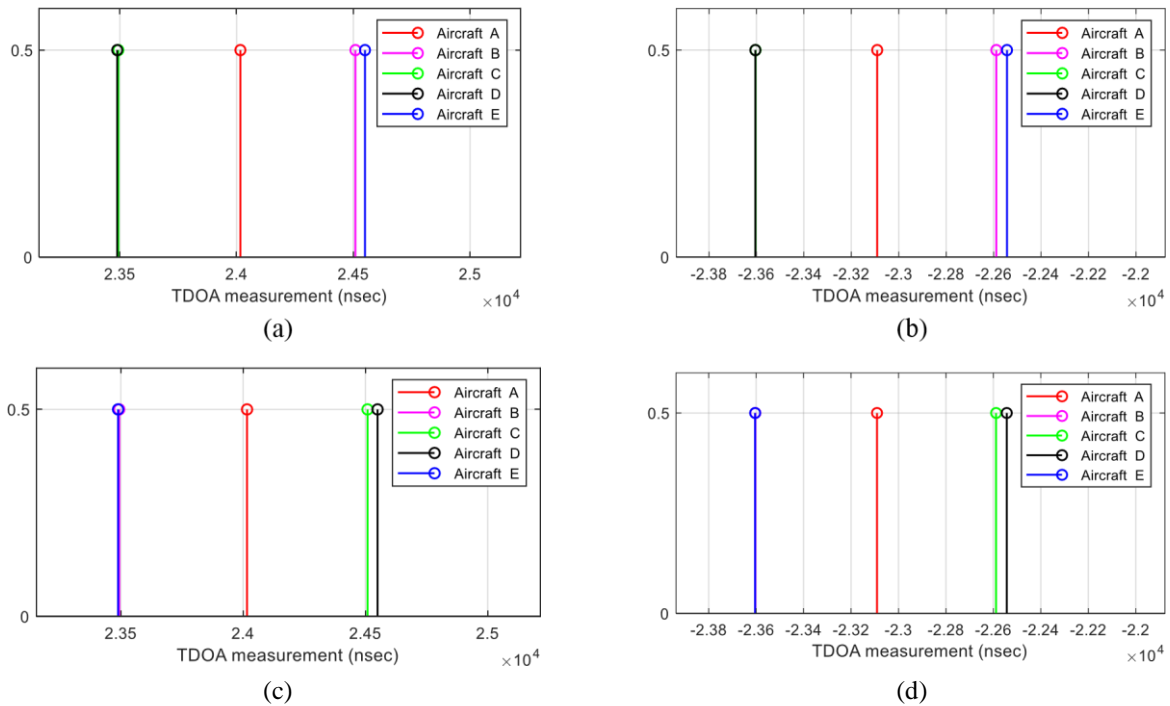


**Fig. 5 - Graphical presentation of TDOA measurement vectors: (a) Vector  $T_{12}$ , (b) Vector  $T_{13}$ , (c) Vector  $T_{42}$ , and (d) Vector  $T_{43}$**

The TDOA measurement pair with the least absolute difference ( $\delta_\tau$ ) have a higher chance of been wrongly associated when estimated in the presence of noise. The TDOA measurements of aircraft C and D from TDOA measurement vectors  $T_{12}$  and  $T_{13}$  have the least absolute difference values of about  $\delta_{12,\tau} = 4.67$  nsec and  $\delta_{13,\tau} = 0.67$  nsec respectively. Likewise, from TDOA measurement vectors  $T_{42}$  and  $T_{43}$ , the TDOA measurements of aircraft B and E have the least absolute difference of about  $\delta_{42,\tau} = 4.67$  nsec and  $\delta_{43,\tau} = 0.67$  nsec. This means that in TDOA measurement vectors  $T_{12}$  and  $T_{13}$ , the

TDOA measurement of aircraft C and D have a higher chance of been wrongly associated so also the TDOA measurements of aircraft B and C in vector  $T_{42}$  and  $T_{43}$ .

In the next section, using the TDOA error SD, the probability of an association error in each of the TDOA measurement vector is determined.

### 4.2 M-RETA Technique Probability of Correct Aircraft Position Estimation

By considering the TDOA measurement pair with the least absolute difference in vector  $T_{12}$  from Fig. 5 which are from the aircraft C and D, the value of  $\delta_{12,\tau} = 4.67$  nsec. The TDOA error SDs at these two aircraft positions from Table 4 using GRS pair 1 are  $\sigma_{12,c} = 2.46$  nsec and  $\sigma_{12,d} = 2.26$  nsec respectively. The result of three times the sum of the two TDOA error SDs is  $3(\sigma_{12,c} + \sigma_{12,d}) = 14.16$  nsec. Since  $\delta_{12,\tau} < 3(\sigma_{12,c} + \sigma_{12,d})$  for the TDOA measurements of aircraft C and D in vector  $T_{12}$ , it means that the overlapping regions given as region A and region B as shown in Fig. 2 are created. Based on Eq. (28), the TDOA association error probability in the TDOA measurement vector  $T_{12}$  that is  $P_{assoc\_err}$  is 3%. This means is that there is a probability of about 3% that two estimated TDOA measurements in vector  $T_{12}$  will be wrongly associated and these measurements are from aircraft C and D.

Extending the analysis to vectors  $T_{13}$ ,  $T_{42}$  and  $T_{43}$ , for the least absolute TDOA measurement differences of  $\delta_{13,\tau} = 0.67$  nsec,  $\delta_{42,\tau} = 4.67$  nsec and  $\delta_{43,\tau} = 0.67$  nsec respectively. The three-time sum of their TDOA error SDs are about 13.59 nsec, 17.10 nsec and 16.56 nsec respectively. For the TDOA measurement vectors  $T_{13}$ ,  $T_{42}$  and  $T_{43}$ , the overlapping region is created, and this will lead to an association error. The TDOA association error probability in the TDOA measurement vectors  $T_{13}$ ,  $T_{42}$  and  $T_{43}$  are obtained as 19%, 4% and 20% respectively. This means that in vectors  $T_{13}$ ,  $T_{42}$  and  $T_{43}$ , there is a probability of about 19%, 4% and 20% that two estimated TDOA measurements in each vector are wrongly associated. In vector  $T_{13}$ , the TDOA measurements are from aircraft C and D while in vectors  $T_{42}$  and  $T_{43}$  the TDOA measurements are from aircraft B and E.

Base on Eq. (31), the probability that PE errors in estimating the positions of each of the aircraft in the flying formation as shown in Fig. 3 is due to an association error by the M-RETA technique is  $P_{PE\_assoc\_error} = 12\%$ . This means that 88% of the time, the PE error obtained by the lateration algorithm coupled with the M-RETA technique is due to the TDOA estimation error. In the next section, using the TDOA error SDs shown in Table 4 for the different aircraft positions and GRS pairs, the estimated aircraft positions using the lateration algorithm in section 3.3 are determined.

### 4.3 Multiple Reference Closed-form Lateration Algorithm Position Estimation Error

The estimated aircraft positions using the TDOA measurements associated by the M-RETA technique in Section 3.1 is determined using the aircraft positions shown in Fig. 3 and the TDOA error SDs shown in Table 4. For each aircraft position, the position root mean square error (RMSE) is obtained after 500 realization Monte Carlo simulation. Fig. 7 shows the estimated and the actual aircraft positions based on the geometrical locations of each aircraft as presented in Fig. 4.

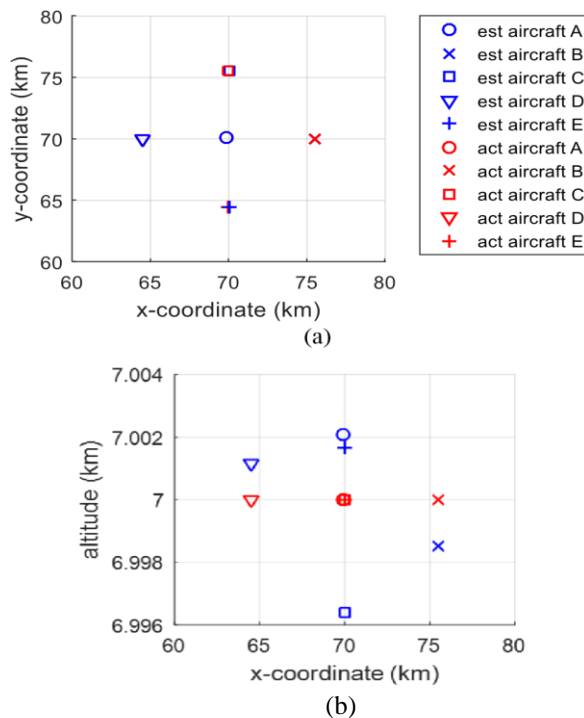


Fig. 6 - Comparison between estimated and actual aircraft position; (a) Horizontal coordinate; (b) Altitude position

From Fig. 6, the position RMSE of the lateration algorithm varies with the aircraft positions. The horizontal position RMSE for aircraft at positions A, B, C, D and E are 3.3 m, 3.5 m, 10 m, 0.8 m and 4.8 m respectively. The altitude RMSE are 0.86 m, 7.4 m, 5.2 m, 3.9 m and 6.8 m for aircraft at positions A, B, C, D and E respectively. Based on the M-RETA performance analysis earlier presented in section 4.2, the deviations in the actual position of each aircraft that is the position RMSE is 12% due an association error and 88% due to TDOA estimation error.

## 5 Conclusion

In this paper, a M-RETA technique is developed for the minimum configuration 3-D multilateration system. The technique is based on multiple reference approach for the TDOA estimation, the cyclic sum property of the TDOA measurements and nearest neighbor search algorithm. The condition for a TDOA measurement association error established based on separation of aircraft and TDOA error SD. The grouped TDOA measurements by the M-RETA technique from 5 aircraft with a minimum horizontal lateral separation of about 5.5 km are used as input to the multiple reference closed-form lateration algorithm. Simulation result shows the position RMSE obtained by lateration algorithm due to an association error by the M-RETA technique is about 12%.

## Acknowledgement

The authors thank Universiti Teknologi Malaysia (UTM) and Ahmadu Bello University for providing the resources and support for this research.

## References

- [1] ICAO. (2007). Guidance Material on Comparison of Surveillance Technologies (GMST). Montreal, Quebec, Canada.
- [2] Kaune, R., Steffes, C., Rau, S., Konle, W., & Pagel, J. (2012). Wide area multilateration using ADS-B transponder signals. In 15th IEEE International Conference on Information Fusion (pp. 727–734). Retrieved from [http://ieeexplore.ieee.org/xpls/abs\\_all.jsp?arnumber=6289874](http://ieeexplore.ieee.org/xpls/abs_all.jsp?arnumber=6289874)
- [3] Shamian, M. Z., Hadi, A., & Ijaz, K. (2012). Ultra-Wide Band Localization and Tracking Hybrid Technique using VRTs. International Journal of Integrated Engineering, 4(3), 65–71. Retrieved from <http://penerbit.uthm.edu.my/ojs/index.php/ijie/article/view/625>
- [4] Galati, G., Leonardi, M., Balbastre-Tejedor, J. V., & Mantilla-Gaviria, I. I. A. (2014). Time-difference-of-arrival Regularised Location Estimator for Multilateration Systems. IET Radar, Sonar & Navigation, 8(5), 479–489. <https://doi.org/10.1049/iet-rsn.2013.0151>.
- [5] Yaro, A. S., & Sha'ameri, A. Z. (2018). Effect of path loss propagation model on the position estimation accuracy of a 3-dimensional minimum configuration multilateration system. International Journal of Integrated Engineering, 10(4), 35–42.
- [6] So, H. C. (2012). Source Localization: Algorithms and Analysis. In B. R. Michael (Ed.), Handbook of Position Location: Theory, Practice, and Advances (1st ed., pp. 25–66). John Wiley & Sons, Inc.
- [7] Yaro, A. S., Sha'ameri, A. Z., & Kamel, N. (2018). Position Estimation Bias Analysis of a Multilateration System with a Reference Station Selection Technique. Advances in Electrical and Electronic Engineering, 16(3), 332–340.
- [8] Chaitanya, D. E., Kumar, M. N. V. S. S., Rao, G. S., & Goswami, R. (2015). Convergence Issues of Taylor Series Method in Determining Unknown Target Location using Hyperbolic Multilateration. International Conference on Science Engineering and Management Research, (1), 1–4. <https://doi.org/10.1109/ICSEMR.2014.7043670>.
- [9] Yaro, A. S., Sha'ameri, A. Z., & Kamel, N. (2017). Ground receiving station reference pair selection technique for a minimum configuration 3D emitter position estimation multilateration system. Advances in Electrical and Electronic Engineering, 15(3), 391–399. <https://doi.org/10.15598/aeec.v15i3.2254>.
- [10] Weng, Y., Xiao, W., & Xie, L. (2011). Total Least Squares Method for Robust Source Localization in Sensor Networks Using TDOA Measurements. International Journal of Distributed Sensor Networks, 7(1), 172902. <https://doi.org/10.1155/2011/172902>.
- [11] Scheuing, J., & Yang, B. (2008). Correlation-Based TDOA-Estimation for Multiple Sources in Reverberant Environments. In Speech and Audio Processing in Adverse Environments (pp. 381–416). Springer, Berlin, Heidelberg. [https://doi.org/10.1007/978-3-540-70602-1\\_11](https://doi.org/10.1007/978-3-540-70602-1_11)
- [12] Jamali-Rad, H., & Leus, G. (2013). Sparsity-Aware Multi-Source TDOA Localization. IEEE Transactions on Signal Processing, 61(19), 4874–4887. <https://doi.org/10.1109/TSP.2013.2272288>.
- [13] Li, H., & Li, C. (2014). TDOA based data association and multi-targets passive localization algorithm. In 7th International Congress on Image and Signal Processing (pp. 1120–1124). Dalian, China, China: IEEE. <https://doi.org/10.1109/CISP.2014.7003948>.
- [14] Amishima, T., Wakayama, T., & Okamura, A. (2014). TDOA Association for Localization of Multiple Emitters when each Sensor Receives Different Number of Incoming Signals. In Proceedings of the SICE Annual Conference (SICE) (pp. 1656–1661). Sapporo, Japan: IEEE. <https://doi.org/10.1109/SICE.2014.6935288>.

- [15] Xionghu Zhong, & Hopgood, J. R. (2015). A Time-Frequency Masking Based Random Finite Set Particle Filtering Method for Multiple Acoustic Source Detection and Tracking. *IEEE Transactions on Audio, Speech, and Language Processing*, 23(12), 2356–2370. <https://doi.org/10.1109/TASLP.2015.2479041>.
- [16] Lee, Y. K., Lee, C. B., Yang, S. H., Lee, J. G., & Hwang, S. W. (2016). Evaluation of Performance Enhancement on CRLB of CAF Under Multiple Emitters. *Electronics Letters*, 52(3), 235–237. <https://doi.org/10.1049/el.2015.2934>
- [17] Herath, S. C. K., Pathirana, P. N., Champion, B. T., & Ekanayake, S. W. (2012). Localization with Ghost Elimination of Emitters via Time-delay-of-arrival Measurements. In 6th International Conference on Information and Automation for Sustainability (pp. 337–341). Beijing, China: IEEE. <https://doi.org/10.1109/ICIAFS.2012.6419928>.
- [18] Xu, X., Chen, W., & Jiang, M. (2013). Multi-target Passive Location based on the Algorithm of TDOA-Camberra. In 25th Chinese Control and Decision Conference (CCDC) (pp. 881–885). Guiyang, China: IEEE. <https://doi.org/10.1109/CCDC.2013.6561047>.
- [19] Sha'ameri, A. Z., Yaro, A. S., Amjad, F. M., & Hamdi, M. N. M. (2017). Performance Comparison of Emitter Locating System for Low Level Airborne Targets. *Defence S and T Technical Bulletin*, 10(3), 199–217. Retrieved from [http://www.stride.gov.my/v1/techbulletin/2017\\_vol\\_10\\_num\\_3.pdf](http://www.stride.gov.my/v1/techbulletin/2017_vol_10_num_3.pdf).
- [20] Marmaroli, P., Falourd, X., & Lissek, H. (2012). A comparative study of time delay estimation techniques for road vehicle tracking. In 11th French Congress of Acoustics and 2012 Annual IOA Meeting (pp. 136–140). Nantes, France.
- [21] Galati, G., Leonardi, M., Mantilla-Gaviria, I. A., & Tosti, M. (2012). Lower bounds of accuracy for enhanced mode-S distributed sensor networks. *IET Radar, Sonar & Navigation*, 6(3), 190. <https://doi.org/10.1049/ietrsn.2011.0197>.
- [22] Mantilla-Gaviria, I. A., Leonardi, M., Galati, G., & Balbastre-Tejedor, J. V. (2015). Localization Algorithms for Multilateration (MLAT) Systems in Airport Surface Surveillance. *Signal, Image and Video Processing*, 9(7), 1549–1558. <https://doi.org/10.1007/s11760-013-0608-1>.
- [23] Chen, Y., Francisco, J. A., Trappe, W., & Martin, R. P. (2006). A Practical Approach to Landmark Deployment for Indoor Localization. In 3rd IEEE Communications Society on Sensor and Ad Hoc Communications and Networks (Vol. 1, pp. 365–373). Reston, VA, USA: IEEE. <https://doi.org/10.1109/SAHCN.2006.288441>.